We are IntechOpen,
the world's leading publisher of
Open Access books
Built by scientists, for scientists

6,900
Open access books available

186,000
International authors and editors

200M
Downloads

154
Countries delivered to

Our authors are among the

TOP 1%
most cited scientists

12.2%
Contributors from top 500 universities

CLARIVATE ANALYTICS
BOOK CITATION INDEX
INDEXED

WEB OF SCIENCE™

Selection of our books indexed in the Book Citation Index
in Web of Science™ Core Collection (BKCI)

Interested in publishing with us?
Contact book.department@intechopen.com

Numbers displayed above are based on latest data collected.
For more information visit www.intechopen.com

Micro Eletro Discharge Milling for Microfabrication

Mohammad Yeakub Ali, Reyad Mehfuz,
Ahsan Ali Khan and Ahmad Faris Ismail
International Islamic University,
Malaysia

1. Introduction

Miniaturization of product is increasingly in demand for applications in numerous fields, such as aerospace, automotive, biomedical, healthcare, electronics, environmental, communications and consumer products. Researchers have been working on the microsystems that promise to enhance health care, quality of life and economic growth. Some examples are micro-channels for micro fuel cell, lab-on-chips, shape memory alloy 'stents', fluidic graphite channels for fuel cell applications, miniature actuators and sensors, medical devices, etc. (Madou, 2002; Hsu, 2002). Thus, miniaturization technologies are perceived as potential key technologies.

One bottleneck of product miniaturization is the lack of simpler and cheaper fabrication techniques. Currently the common techniques are based on silicon processing techniques, where silicon-based materials are processed through wet and dry chemical etching. These techniques are suitable for microelectronics, limited to few silicon-based materials and restricted to simple two dimensional (2D) or pseudo three dimensional (2.5D) planar geometries. Other fabrication processes, such as LiGA (lithography, electroforming and molding), laser, ultrasonic, focused ion beam (FIB), micro electro discharge machining (EDM), mechanical micromilling, etc. are expensive and required high capital investment. Moreover these processes are limited to selected materials and low throughput (Ehmann et al. 2002).

A less expensive and simpler microfabrication technique is sought to produce commercially viable microcomponents. Micro electro discharge (ED) milling, a new branch of EDM, has potential to fabricate functional microcomponents. The influences of micro ED milling process parameters on surface roughness, tool wear ratio and material removal rate are not fully identified yet. Therefore, modeling of ED milling process parameters for surface roughness, tool wear ratio and material removal rate are necessary.

1.1 Micro electro discharge machining

EDM has been successfully used for micromachining with high precision regardless of the hardness of work piece material. It uses the removal phenomenon of electrical discharges in a dielectric fluid. Two conductive electrodes, one being the tool and the other the workpiece, are immersed in a liquid dielectric. A series of voltage pulses are applied between the electrodes, which are separated by a small gap. A localized breakdown of the dielectric

occurs and sparks are generated across the inter-electrode gap, usually at regions where the local electric field strength is highest. Plasma channels towards workpiece are formed during the discharge and high speed electrons come into collision with the workpiece. Each spark erodes a small amount of work material by melting and vaporizing from the surface of both the electrodes. The momentary local plasma column temperature can reach as high as 40,000 K (DiBitonto et al., 1989).
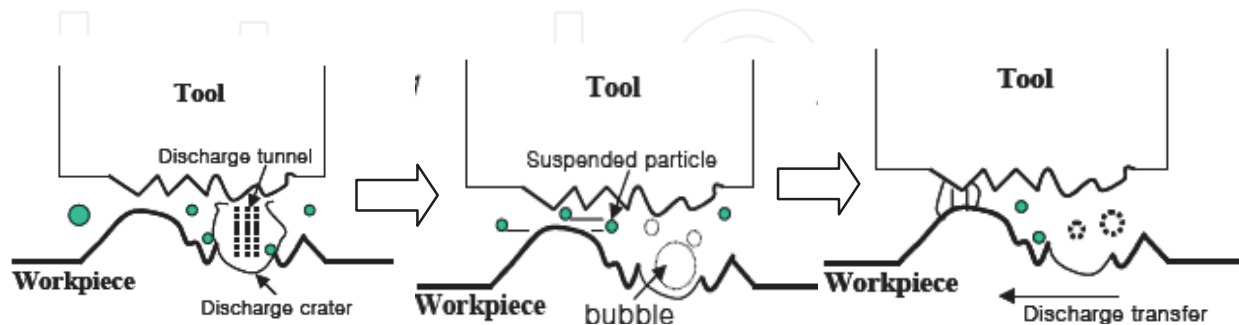

Fig. 1.1. Schematic of EDM principle (Kim et al., 2005)

This high temperature causes the melting and vaporization of the electrode materials; the molten metals are evacuated by a mechanical blast, resulting in small craters on both the tool electrode and work materials. It is understood that the shock waves, electromagnetic and electrostatic forces involved in the process are responsible for ejection of the molten part (debris) into the dielectric medium. The repetitive impulse together with the feed movement (by means of a servo mechanism) of the tool electrode towards the workpiece enables metal removal along the entire surface of the electrodes. Figure 1.1 shows the schematic of EDM principle.

Production of micro-features using EDM pays significant attention to the research community. This is due to its low set-up cost, high accuracy and large design freedom. Compared to lithography based miniaturization, micro EDM has the clear advantages in fabricating complex 3D shapes with higher aspect ratio (Lim et al., 2003). Moreover, all conductive materials regardless of hardness can be machined by EDM. Conventional EDM is especially useful to produce molds and dies. Micro EDM is now basically focused on the fabrication of miniaturized product, like molds and dies, with greater surface quality. In this endeavor new CNC systems and advanced spark generators are found as great assistance (Pham et al., 2004). Current micro EDM technology used for manufacturing micro-features can be categorized into four different types:

a) Die-sinking micro-EDM, where an electrode with micro-features is employed to produce its mirror image in the workpiece.
b) Micro-ED drilling, where micro-electrodes (of diameters down to 5–10 μm) are used to 'drill' micro-holes in the workpiece.
c) Micro-ED milling, where micro-electrodes (of diameters down to 5–10 μm) are employed to produce complex 3D cavities by adopting a movement strategy similar to that in conventional milling.
d) Micro-wire EDM, where a wire of diameter down to 20 μm is used to cut through a conductive workpiece.

Precision micro holes required for gas and liquid orifices in aerospace and medical applications, pinholes for x-ray and nuclear fusion measurements, ink-jet printer nozzles and electron beam gun apertures can be fabricated with high precision accuracy and with

surface roughness less than 0.1 μm using the micro EDM process (Dario et al., 1995). Although micro EDM plays an important role in the field of micromachining, it has disadvantages such as high tool-electrode wear ratio and low *MRR*. The wear of electrode must be compensated either by changing the electrode or by preparing longer electrode from the beginning or fabricating the electrode in situ for further machining (Asad et al., 2007).

1.1.2 Micro electro discharge milling

In micro ED milling the material is eroded by non-contact thermo-electrical process, where a series of discrete sparks occur between the workpiece and the rotating tool electrode. The workpiece and tool are immersed in a dielectric fluid. The dielectric fluid is continuously fed to the machining zone to convey the spark and flush away the eroded particles. The work feeding system of micro ED milling is similar to mechanical end milling process. Like mechanical end milling, here the workpiece is fed to the tool electrode while the tool is in rotation. The tool movement is controlled numerically to achieve the desired three-dimensional shape with high accuracy. Figure 1.2 shows the schematic of micro ED milling.
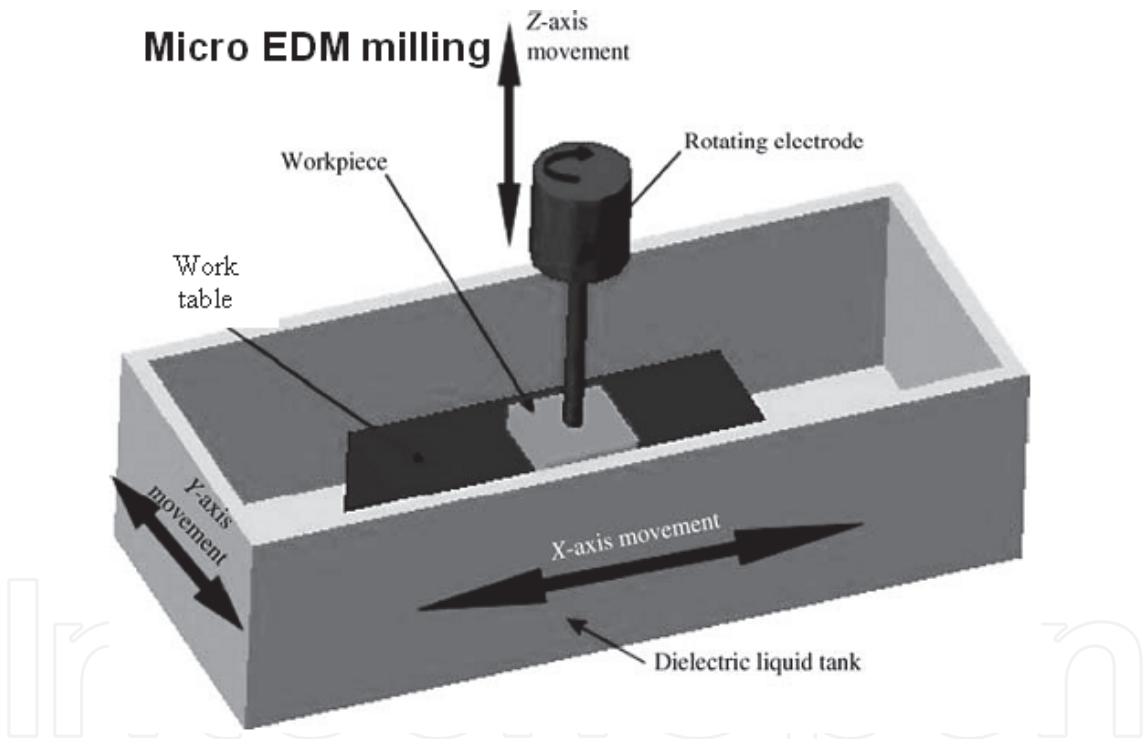

Fig. 1.2. Schematic of micro ED milling (Murali and Yeo, 2004)

Process parameters	
Open voltage	Pulse on time
Capacitance	Pulse off time
Discharge current	Pulse frequency
Resistance	Tool rotation speed
Feed rate	Dielectric flow rate
Polarity	

Table 1.1. Micro ED milling process parameters

1.1.3 Process parameters

Micro ED milling has a number of process parameters, which are influential on the machining performance. Depending upon the circuit type used in the machine, the importance of parameters is also varied. Table 1.1 shows different micro ED milling process parameters. Some researches were conducted to optimize different EDM process parameters for R_a, R_y, TWR and MRR (Puertas and Luis, 2004; Lin et al., 2006). But almost all of them were on conventional macro EDM. Because of the stochastic thermal nature of the EDM process, it is difficult to explain all of those effects fully. The full understanding of micro ED milling process parameters are yet to be developed because the process itself is a new branch of manufacturing. For electric discharge the discharge energy (E) generated in the discharge circuit can be expressed roughly as follows:

$$E = \frac{1}{2}(C + C^{'})V^2 \tag{1.1}$$

Where,
C = capacitance of capacitors,
C' = total stray capacitance,
V = discharge voltage

According to the equation (1.1), there are two ways to reduce the discharge energy: by reducing the discharge voltage or by reducing the total capacitance (C + C'). However, low voltage results in an unstable discharge. Therefore, the total capacitance should be controlled primarily. The total stray capacitance (C') in the circuit plays a significant role here. The following subsections discuss the influence of different micro ED milling parameters on surface roughness, tool wear and material removal rate.

1.1.4 Surface roughness

Variation of discharge energy affects surface roughness. It is experimentally identified that with the increase in discharge energy either by increasing voltage or capacitance, R_a increased in die sinking EDM, wire EDM (WEDM) and WEDG (Uhlmann et al., 2005; Han et al., 2006; Chiang, 2007). A large discharging energy usually causes violent sparks and results a deeper erosion crater on the surface. Accompanying the cooling process after the spilling of molten metal, residues remain at the periphery of the crater to form a rough surface (Liao et al., 2004). Theoretical model for R_y or R_{max} was developed for transistorized pulse generator type EDM (Chen and Mahdivian, 2000). It showed that with the increase in current and pulse duration, R_y increased. Surface roughness of ceramic due to EDM was also investigated. EDM of boron carbide (B_4C) showed that R_a and R_y increased with pulse duration but decreased with current (Puertas and Luis, 2004). On the other hand, EDM of high speed steel showed that with the increase of current, R_a increased and with the increase of pulse duration it decreased (Lin et al., 2006). It was suggested to use low conductive or higher resistive dielectric to ensure low R_a and R_y (Liao et al., 2004). Use of rotating electrode was helpful for high shape accuracy and higher MRR but it caused higher surface roughness (Her and Weng, 2001).

Formation of crack is a challenge in EDM. The presence of high crack density is not desirable because it leads early product failure. Investigation of EDM parameters showed that higher pulse-on duration increased both the average white layer thickness and the induced stress (Lee and Tai, 2003; Ekmekci et al., 2005). These two conditions tend to

promote crack formation. When the pulse current was increased, the increase in material removal rate caused a high deviation of thickness of the white layer. Thus with the increase in pulse current, crack formation decreased. It was also verified that lower thermal conductivity of workmaterial caused higher crack formation. There was no analysis reported on the effect of feed rate on machined surface.

1.1.5 Tool wear

Tool wear is responsible for shape inaccuracy and dimensional instability. In micro ED milling at higher feed rate tool wear was found decreasing (Lim et al., 2003). It was also observed that tool wear was increasing with feed rate but after reaching the peak it started decreasing (Kim et al., 2005). High discharge energy usually caused high *TWR* (Uhlmann et al., 2005). In EDM of high speed steel and boron carbide (B_4C), tool wear was found to be proportional to current and inversely proportional to pulse duration (Puertas and Luis, 2004; Lin et al., 2006). It was also found that tool wear showed an optimum peak value while pulse duration had increased (Ozgedik and Cogun, 2006). However, use of shorter pulse on-time was suggested to achieve lower *TWR* (Son et al., 2007).

The negative polarity of the tool gives a lower tool wear than that of positive polarity in the range of low to medium discharge current values. At high current settings, the polarity has no significant effect on the tool wear. A slight decrease in *TWR* was observed with increasing current in negative polarity. In the case of positive polarity, *TWR* decreased significantly with increasing current (Lee and Li, 2001).

The type of dielectric fluid is also responsible for tool wear rate. Kerosene is frequently use as the dielectric medium. In EDM, carbide layer formed on the workpiece surface with the use of kerosene, which has a higher melting temperature than the oxide layer formed with the use of distilled water. The carbide layer formed by kerosene needed higher pulse energy for melting and evaporation which caused high tool wear (Chen et al., 1999). The use of low resistive deionized water as a dielectric fluid reduced the tool wear as compared to kerosene (Chung et al., 2007).

1.1.6 Material removal rate

Experimental investigation in conventional EDM found that *MRR* increased with the discharge current. With the increase in pulse duration MRR showed a peak and then downfall (Chen and Mahdivian, 2000; Lin et al., 2006;). Increase in discharge energy by discharge voltage or capacitance, resulted in higher *MRR* (Kim et al., 2005). It was also observed that material removal depth was inversely proportional to feed rate (Lim et al., 2003). *MRR* can be increased in both positive and negative polarity by rotating the tool-electrode (Her and Weng, 2001). Higher *MRR* was obtained for low ultrasonic vibration frequency combined with tool rotation (Ghoreishi and Atkinson, 2002).

Dielectric flushing system is also responsible for the variation in *MRR*. The low material removal rate in static condition is mainly due to improper flushing of the molten and evaporated workpiece material from the machining gap (Ozgedik and Cogun, 2006). With the increase in flushing flow rate, *MRR* increased. Use of kerosene and tap water as the dielectric fluid showed higher *MRR* than distill water (Chen et al., 1999).

1.1.7 Tool electrode

EDM tool electrodes should be conductive. A list of different tool electrode materials is shown in Table 1.2. In micro range, the replacement of tool during machining is

unacceptable because it leads to positional inaccuracy. For this, tool with low wear ratio are needed in micro EDM. Because of its low wear ratio, tungsten or tungsten carbide rods or tubes of diameters within the range 100-400 μm are preferred as tool electrodes for micro ED drilling and milling (Pham et al., 2004). The handling of tungsten and tungsten- carbide rods is difficult as they can be easily damaged. Therefore, sub-systems are incorporated into micro EDM machines for on-the-machine manufacture and holding of the required micro-electrodes. The most common sub-systems are ceramic guides and dressing units such as WEDG.

Electrode material	Volume wear ratio (tool/workpiece)	Machinability	Cost	Best application
Brass	1 : 1	Easy	Low	Holes, slits
Copper	1 : 2	Easy	Moderate	Holes
Copper-Tungsten	1 : 8	Moderate	High	Large areas
Zinc	1 : 2	Easy	Low	Die cavities on steel
Steel	1 : 4	Easy	Low	Through holes into non-Fe materials
Tungsten	1 : 10	Poor	High	Small slots, holes
Tungsten carbide	1 : 10	Poor	High	Small slots, holes

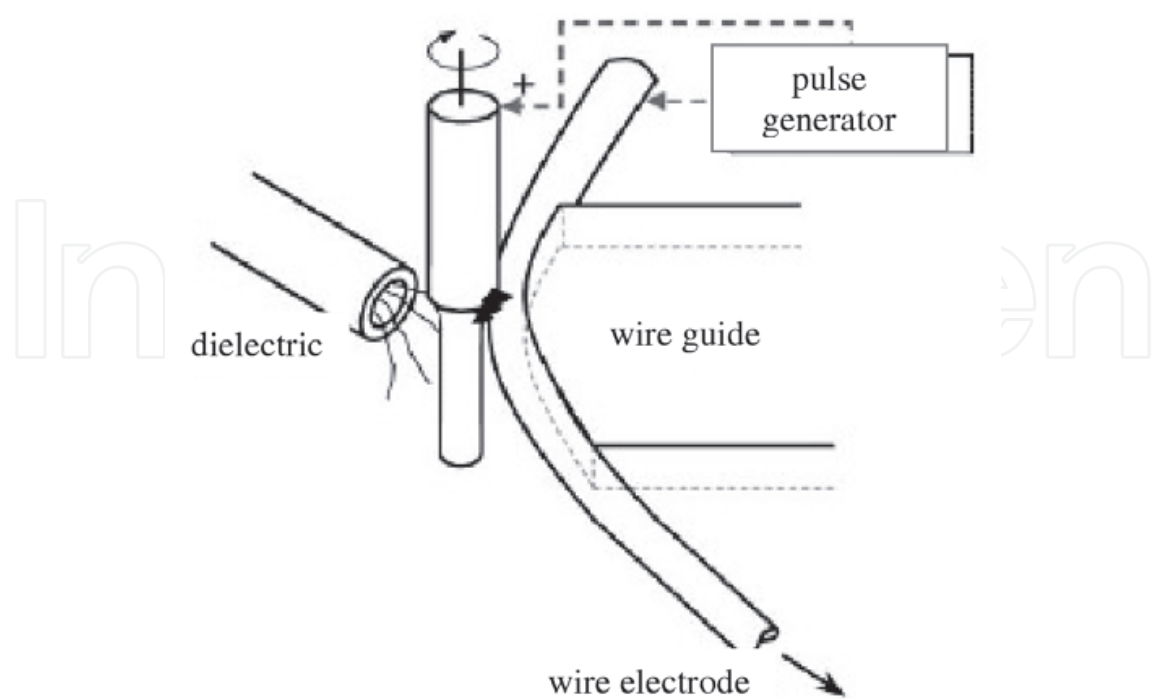Table 1.2. Features of different tool electrode materials

Fig. 1.3. Principle of WEDG with one wire guide (Fleischer et al., 2004)

The tool electrode can be dressed or prepared either by etching, grinding or lithography process. However, when the fabricated tool is chucked on the machine, an alignment error between tool center and spindle center and run-out error of tool which has an influence on the variation of the discharge gap occurs and cause serious problems in micro machining and assembly of micro parts. For this, on-machine tool dressing is always recommended. WEDG is an on-machine tool dressing method. The principle of WEDG was developed in the mid 1980s. The WEDG process is using a traveling wire between one or two guides. The wire is the tool electrode of 50 and 200 μm diameter. In Figure 1.3 the principle of the WEDG-unit with one wire guide is shown, where rotating workpiece is fed downwards and the discharge area is limited to the front edge of the wire. The straightness of the ground part depends only on the variation of the gap distance at the machining point. Minimum 5.5 μm tool was fabricated by WEDG from experiment (Kim et al., 2005). But in WEDG it is difficult to control the shape, dimension and roughness of the ground electrode (Lim et al., 2003).

1.1.8 Workpiece materials

In general, all conductive materials can be machined by the process that follows EDM principle. Different work materials for EDM are as follows:

a) Metals: copper, iron, alloys etc.
b) Semiconductor materials: silicon (Madou, 2002)
c) Conductive ceramics: Alumina, Zirconia, Silicon Nitride, Boron Carbide (Puertas and Luis. 2004; Schoth et al., 2005)
d) Conductive polymers (King et al., 1999) Metal matrix composites (Xingchao, Z et al., 2007)

2. Experimental design

The experiment was designed based on 3-level full factorial statistical model, where the three micro ED milling process parameters were feed rate, capacitance and voltage. The experiment was designed to analyze the individual influences, interaction effects and quadratic effects of these parameters on R_a, R_y, TWR and MRR. Table 2.1 shows the experimental conditions. Total number of 32 experiments had been conducted to complete the analysis. Six experiments at the same combination were conducted to reduce the curvature effect. The response parameters were statistically analyzed by applying factorial ANOVA at probability value of 0.05. This experimental study has been briefly published before (Mehfuz and Ali, 2009)

The definition of response parameters are as follows:

R_a *(μm)= The arithmetic average deviation from the mean line*

R_y *(μm)= Maximum peak-to-valley roughness height*

$$TWR = \frac{Volume\ of\ tool\ wear}{Volume\ of\ workpiece\ wear}$$

$$MRR\ (mg\ /\ min) = \frac{Weight\ of\ material\ removed}{Machining\ time}$$

Controlled Parameters		Experimental conditions		
		Level		
	Factors	*1*	*2*	*3*
Feed rate (μm/s)	A	2.00	4.00	6.00
Capacitance (nF)	B	0.10	1.00	10.00
Voltage (volts)	C	80	100	120

Fixed Parameters	Experimental conditions
Tool electrode	Tungsten
workpiece	Be-Cu alloy
Tool electrode dia (mm)	0.50
Spindle speed (rpm)	2000
Polarity	Workpiece +
Dielectric fluid	EDM-3 (synthetic oil)
Machining length (mm)	13.00
Machining depth (mm)	0.20

Table 2.1. Experimental Conditions of micro ED milling

2.1 Tool and workpiece materials

The workpiece material was beryllium-copper (Be-Cu) alloy (Be = 0.4 %, Ni = 1.8 % Cu = 97.8 %), which is industrially known as Protherm. Some features of Be-Cu alloy are as follows:

a) High thermal conductivity (245.00 W/m^{o}C at 20°C).
b) Resistance to high temperature.
c) Excellent corrosion resistance, which enables it to become a suitable mold material.
d) Good machinability and polishability.

The tool electrode material was tungsten (W). It has the following features:

a) Low tool wear ratio,
b) Suitable for small holes or slot,
c) High cost,
d) Machinable by WEDG.

2.2 Experimental procedures and measurements

In this subsection the equipments used to conduct the experiments and the experimental procedures are described. A commercial multi-purpose miniature machine tool (DT-110 Mikrotools, Singapore), shown in Figure 3.1, was used to conduct the micro ED milling experiments. The machine contained RC circuit to generate small but high frequency

discharge energy. EDM-3 synthetic oil was used as the dielectric fluid. The following subsections discuss the different steps of the experiments.

2.2.1 Sample preparation

Before the experiments, the workpieces were prepared by grinding and polishing. Workpieces were ground by using (NAGASEI SGW 52, Japan) surface grinding machine. Next, the workpiece was grounded manually by using 240, 320, 400 and 1000 grade of sand papers respectively. Then the workpieces were polished by 3 μm diamond suspensions and lubricant. The polishing steps were needed to obtain mirror surface finish. After the final polishing, the workpiece were immersed in acetone and cleaned for 15 minutes by ultrasonic cleaning machine, (BRANSON 2510). Tungsten tool electrodes of 500 μm diameter were also cleaned by the same ultrasonic cleaning machine to clean. Ultrasonic cleaning is useful for the removal of micro sized dirt particle. Then both the workpieces and tool-electrodes were weighed on an electric balance (B204-S Mettler Toledo, Switzerland) with a resolution of 0.1 mg. The measured weights before and after machining were compared. The following shows the specifications of a sample workpiece and tool-electrode after the final polishing. The prepared samples were then used for micro ED milling as discussed in following subsection.

Specification of the workpiece:

Thickness = 5 mm
Length = 50 mm
Width = 15 mm

Specification of the tool-electrode:

Diameter = 500 μm
Length = 50 mm

2.2.2 Experiments by micro electro discharge milling

At the beginning of the micro ED milling set-up, the tool electrode was clamped in the spindle, while the workpiece was clamped on the worktable. After clamping, the spindle rotation was fixed at a speed of 2000 rpm, the worktable was fed and dielectric fluids were flown to the sparking zone. When discharge occurred between the tool-electrode and the workpiece, a small portion of workpiece melted and evaporated due to high local temperature, creating a crater on the work surface. The workpiece cooled rapidly by the influence of dielectric fluid. Figure 2.1a schematically depicts the experimental setup. The experiment was done to fabricate a microchannel for the dimensions of 13 mm length, 0.5 mm width and 0.2 mm depth. Figure 2.1b shows the schematic of the microchannels after micro ED milling. Computer numerical coding was used to conduct the experiment. The machining time was obtained from the auto stopwatch of the integrated computer. After the experiment, both the tool-electrode and workpiece were cleaned again in ultrasonic cleaning bath and dried.

After this, the tool-electrode and workpiece were weighed to find out the weight loss due to machining. The differences of weight before and after machining were used to calculate the *TWR* and *MRR*. After weighing, the samples were put into a dry box to avoid the moisture

contact. These samples were used for SEM investigation and measurement of R_a and R_y as discussed in the following subsections.
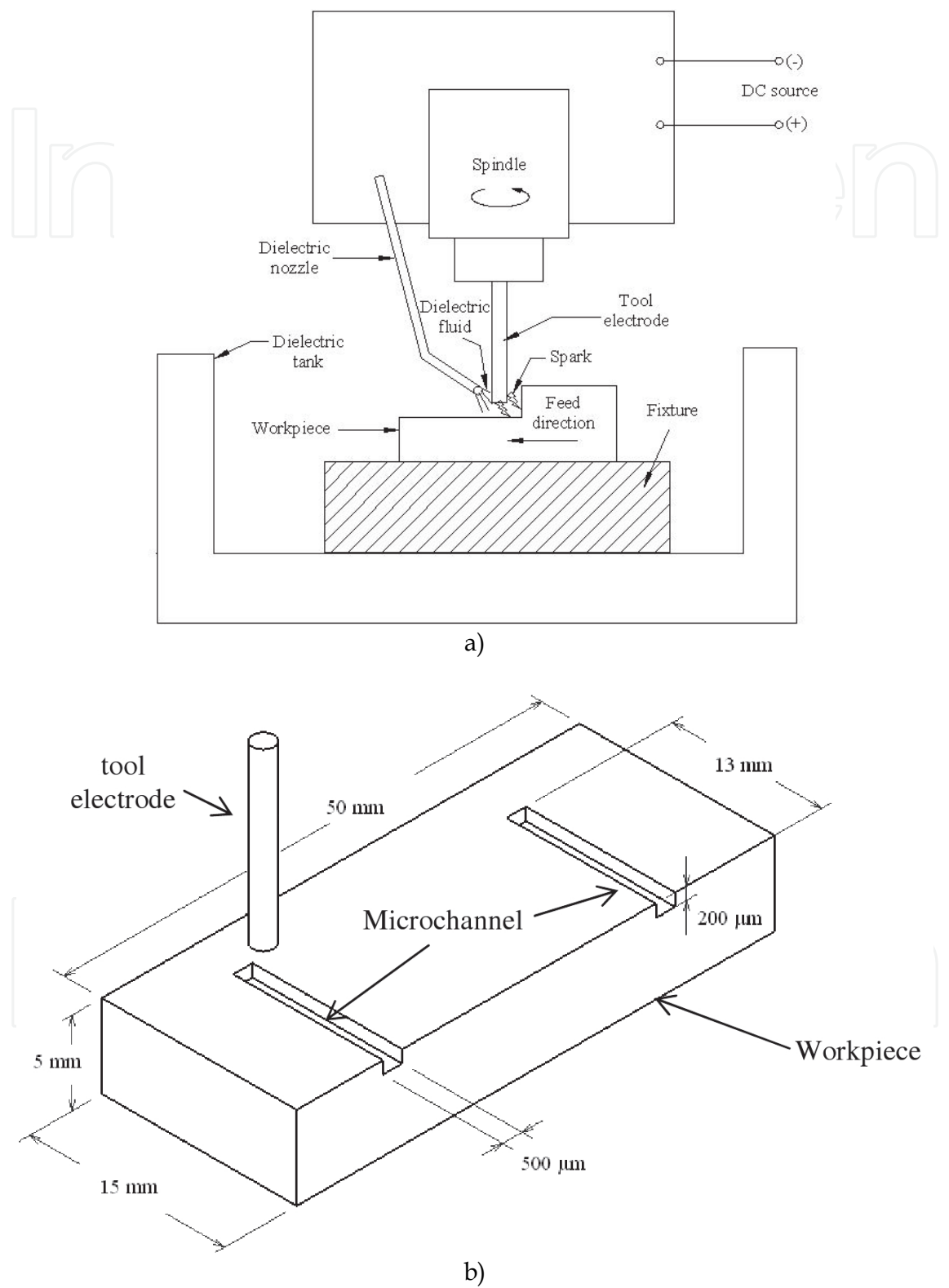

a)

b)

Fig. 2.1. Schematic of experiment: (a) micro ED milling process, (b) specification of the microchannel

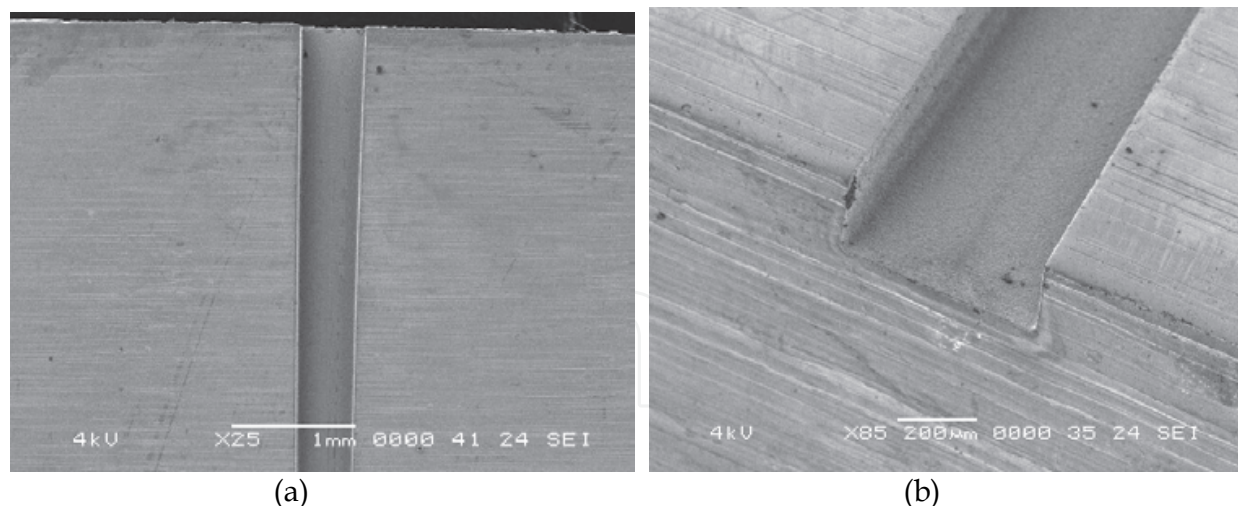(a)   (b)

Fig. 2.2. SEM micrographs of a microchannel, a) top view, b) isometric view

2.2.2.1 SEM Inspection

The work sample was cleaned by ultrasonic cleaning and sputter coated with carbon by Coater (SC 7640). Though the work material was conductive, it was coated to get high quality images. The machined surfaces were then inspected by scanning electron microscope (SEM) (JEOL JSM-5600). Figure 2.2 shows SEM micrographs of a microchannel produced by micro ED milling.

2.2.2.2 Measurement of surface roughness

Both the R_a and R_y were measured by using a precision surface profiler (Mitutoyo, Surftest SV-500, Japan). This profiler provided surface roughness along a line with a resolution of 10 nm. As the length of the microchannel was 13 mm long, the roughness was measured in three segments. Each segment was 3.5 mm long. Average of these three measurements was taken as the surface roughness value.

3. Results and discussions

The experimental results of R_a, R_y, *TWR* and *MRR*, are analyzed using variance approach (ANOVA) to check the adequacy of the developed statistical model. The analysis ultimately showed the main and interaction effects of the process variables on the responses. Main effect was the direct effect of an independent variable while interaction effect was the joint effect of two independent variables on the response.

3.1 Calculation of analysis of variance

ANOVA is a calculation procedure to allocate the amount of variation in a process and determine if it is significant or is caused by random noise. ANOVA tables are constructed for R_a, R_y, *TWR* and *MRR* respectively. The statistical significance of each effect by means of the comparison of the mean squares (MS) with an estimation of the experimental error was performed. In the table, SS represents sum of squares while DF represents the number of degrees of freedom. The column corresponding to MS is obtained simply by dividing SS by its corresponding DF. In contrast, column of F value is calculated as the quotient of each of the MS of the effects divided by the value of the MS corresponding to the residual. Column of

Exp No.	Feed rate (μm/s)	Capacitance (nF)	Voltage (volt)	R_a (μm)	R_y (μm)	TWR	MRR (mg/min)
1	2.00	0.10	80.00	0.04	0.31	0.121	0.02
2	4.00	0.10	80.00	0.04	0.35	0.044	0.07
3	6.00	0.10	80.00	0.04	0.36	0.133	0.09
4	2.00	1.00	80.00	0.10	0.78	0.154	0.04
5	4.00	1.00	80.00	0.12	0.91	0.066	0.09
6	6.00	1.00	80.00	0.10	0.89	0.165	0.09
7	2.00	10.00	80.00	0.44	3.23	0.182	0.06
8	4.00	10.00	80.00	0.44	3.21	0.089	0.10
9	6.00	10.00	80.00	0.48	3.53	0.220	0.11
10	2.00	0.10	100.00	0.05	0.49	0.165	0.03
11	4.00	0.10	100.00	0.05	0.40	0.049	0.09
12	6.00	0.10	100.00	0.06	0.54	0.157	0.09
13	2.00	1.00	100.00	0.19	1.28	0.194	0.06
14	4.00	1.00	100.00	0.17	1.20	0.065	0.16
15	6.00	1.00	100.00	0.18	1.38	0.186	0.14
16	2.00	10.00	100.00	0.53	3.99	0.239	0.10
17	4.00	10.00	100.00	0.54	4.08	0.098	0.35
18	6.00	10.00	100.00	0.53	4.05	0.216	0.13
19	2.00	0.10	120.00	0.05	0.44	0.198	0.06
20	4.00	0.10	120.00	0.07	0.52	0.065	0.15
21	6.00	0.10	120.00	0.08	1.23	0.166	0.10
22	2.00	1.00	120.00	0.19	1.81	0.227	0.07
23	4.00	1.00	120.00	0.17	1.22	0.086	0.36
24	6.00	1.00	120.00	0.18	1.37	0.198	0.14
25	2.00	10.00	120.00	0.56	3.11	0.261	0.16
26	4.00	10.00	120.00	0.62	3.79	0.128	0.41
27	6.00	10.00	120.00	0.54	3.77	0.247	0.15
28	4.00	1.00	100.00	0.22	1.30	0.058	0.10
29	4.00	1.00	100.00	0.22	1.53	0.072	0.49
30	4.00	1.00	100.00	0.15	1.06	0.067	0.24
31	4.00	1.00	100.00	0.19	1.47	0.062	0.13
32	4.00	1.00	100.00	0.16	1.28	0.075	0.20

Table 3.1. Design matrix of the experiment and measured responses

Probability values gives the probability values associated with values that take the variable of a function of distribution F.

$$SS_{total} = SS_{error} + SS_{treatments}$$

$$SS_{total} = SS_{error} + SS_{treatments}$$

$$SS_{total} = SS_{error} + SS_{treatments}$$

$$Model\ F-value = \frac{MS\ model}{MS\ residual}$$

3.1.1 Surface roughness

Table 3.2 shows the analysis of variance for R_a. Using this analysis a second order quadratic model was developed, which is shown below in Equation (3.1). The model was developed for 95% level of confidence. The model F-value of 213.06 implies the model is significant. There is almost no influence, 0.01%, of noise on the model developed. By checking F value and P-value it is clearly seen that Factor B (capacitance), Factor C (voltage) and Factor B^2 are most influential on R_a. The P-value of each of these factors indicates the confidence level is more than 99.00%, which shows their very strong influence. The P - value of interaction effects of BC shows the confidence level is above 95.0% and thus shows very good influence on R_a. The P-value of Factor A (feed rate) and interaction Factor AC has insignificant influence over R_a as it provides very high P values. The lack of fit F-value of 0.53 implies that the lack of fit is not significant compare to the pure error. The high P-value of lack of fit, 85.35%, indicates the model is fit, while the very low P-value of the model, 0.01%, indicates that the model is significant. The specific power transformation was chosen within the confidence level, which was suggested by the Design Expert software toolbox using Box-Cox plotting. In this case, natural log power transformation was suggested. Thus the developed statistical quadratic equation for R_a is:

$$Ln(R_a) = -7.956 - 0.044f + 1.423C + 0.087V - 0.111C^2 - 0.0004V^2 + 0.0006fV - 0.0007CV \qquad (3.1)$$

Source	SS	DF	MS	F Value	Prob > F	For 95% level of confidence
Model	24.88	7	3.55	213.06	< 0.0001	significant
A	0.02	1	0.02	1.18	0.2885	
B	23.82	1	23.82	1427.90	< 0.0001	
C	0.59	1	0.59	35.44	< 0.0001	
B2	4.69	1	4.69	281.06	< 0.0001	
C2	0.17	1	0.17	10.47	0.0035	
AC	0.01	1	0.01	0.43	0.5194	
BC	0.07	1	0.07	4.42	0.0461	
Residual	0.40	24	0.02			
Lack of Fit	0.27	19	0.01	0.53	0.8535	not significant
Pure Error	0.13	5	0.03			
Cor Total	25.28	31				

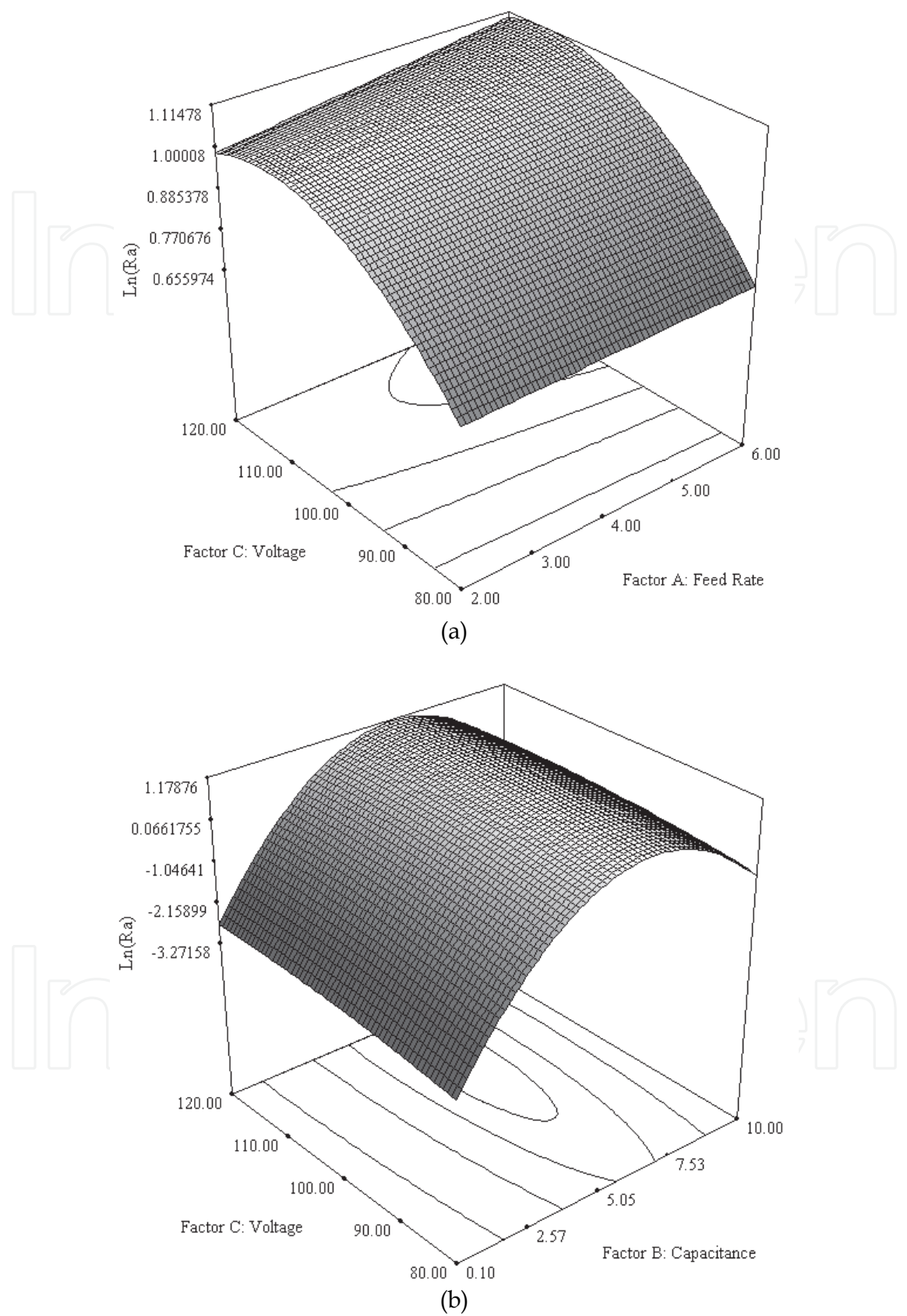Table 3.2. Analysis of variance for main and interaction effects on R_a

(a)

(b)

Fig. 3.1. Estimated response surface of R_a (µm): (a) $Ln(R_a)$ vs. f and V when C = 1.0 nF, (b) $Ln(R_a)$ vs. C and V, when f = 4.0 µm/s

Figure 3.1 shows the effect of feed rate-voltage and capacitance-voltage on R_a respectively. Capacitance and voltage are strongly influential on R_a. R_a increases along with the increase in voltage, which is same as the conventional EDM. With the increase of capacitance from 0.1 to 5 nF the R_a value increases but for further increase of capacitance the R_a values reduce. As the capacitance increased, large energy dissipated which erodes more materials with stronger spark. This strong spark erodes materials with high amount of debris from both the tool electrode and workpiece creating uneven crater. As these debris are trapped in between the plasma channel, it causes unwanted spark. Thus, a high amount of discharge energy is employed to spark with debris, while work material is effectively removed by a small portion of discharge energy. Thus lower R_a is obtained.
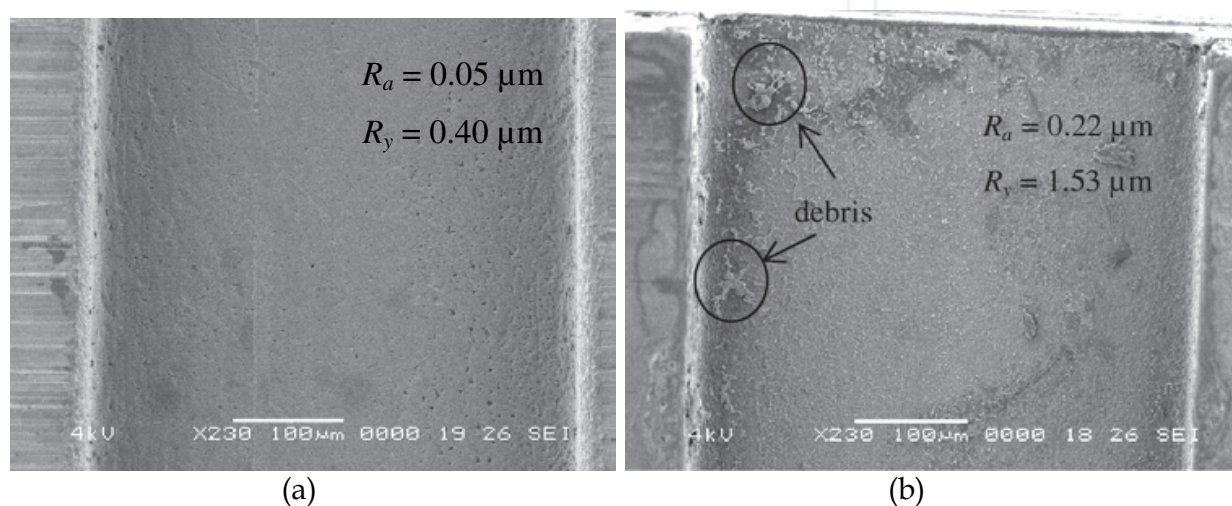
Fig. 3.2. SEM micrograph of the surface texture of micro ED milled surface when feed rate = 4 µm/s and voltage = 100 volts, with varying capacitance of (a) 0.1 nF and (b) 1.0 nF.

Figure 3.2 shows SEM surface texture of two machined surfaces with varying capacitance. In the Figure 4.2a the surface texture was found very smooth (R_a = 0.05 µm) with 0.1 nF capacitance. Figure 4.2b shows the surface texture (R_a = 0.22 µm) with the capacitance of 1 nF. Here, the surface was found rougher with increased amount of unwashed debris.
Similarly the developed statistical quadratic equation for maximum peak-to-valley height roughness, R_y is:

$$Ln(R_y) = -4.981 - 0.077f + 1.264C + 0.07V - 0.091C^2 - 0.0003V^2 + 0.0012fV - 0.0014CV \quad (3.2)$$

3.1.2 Tool Wear Ratio

A second order quadratic model was developed which is the mathematical expression of TWR:

$$TWR = 0.285 - 0.203f + 0.031C + 0.002V + 0.029f^2 - 0.003C^2 +$$
$$0.0002fC - 0.0003fV \quad (3.3)$$

Figure 3.4 shows the effect of feed rate-capacitance and feed rate-voltage on *TWR*. Capacitance and voltage are found as the strong influencer of *TWR*, like R_a, along with the

(a)

(b)
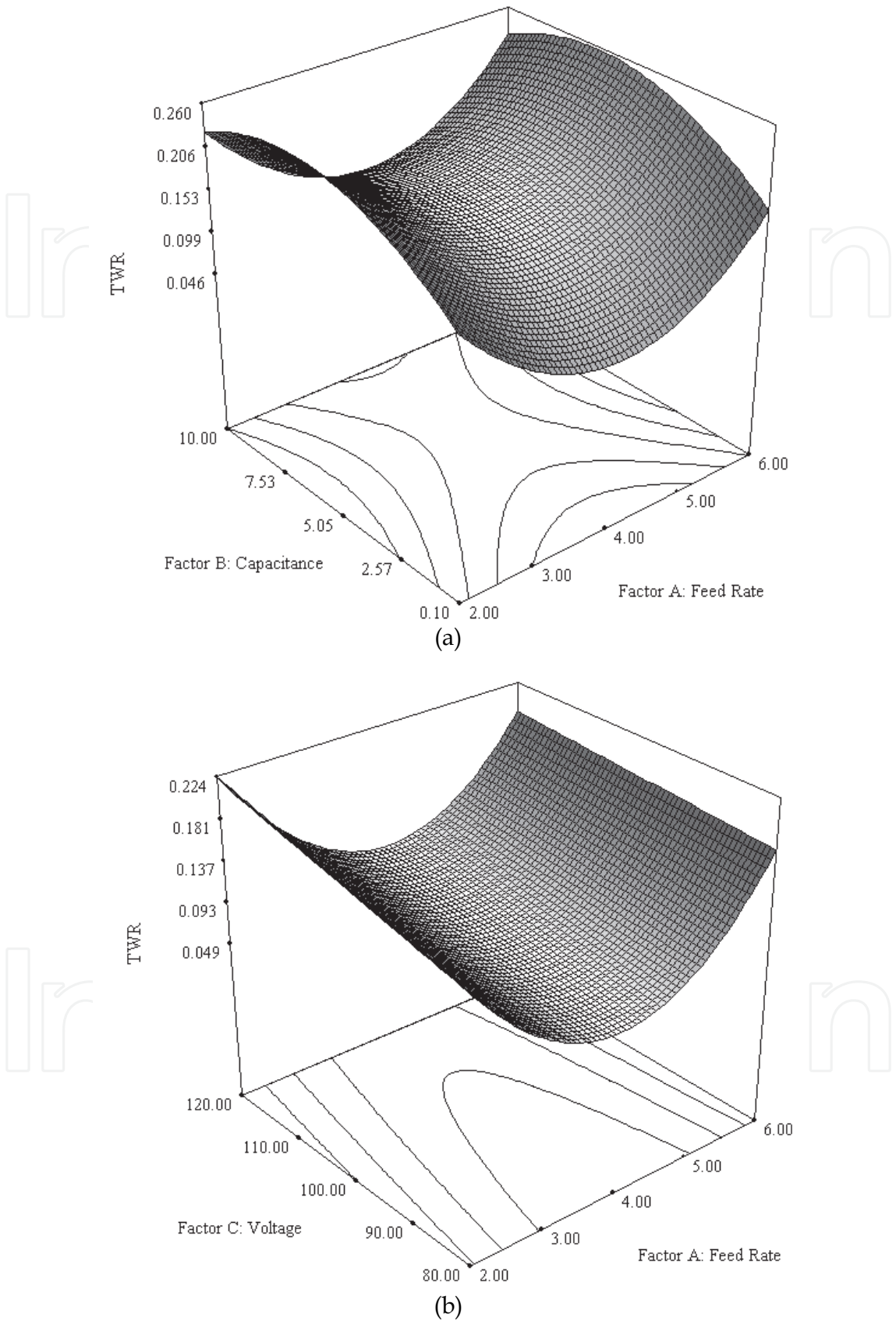
Fig. 3.4. Estimated response surface of *TWR*: (a) *TWR* vs. *f* and *C* when *V* = 100 volts,
(b) *TWR* vs. *f* and *V*, when C = 1.0 nF

interaction effect of feed rate-voltage. *TWR* decreases with the increase in feed rate. For further increase in feed rate *TWR* starts rising. In the first phase, for a particular spark energy discharge if the feed rate is so small it will have high electron emission rate from the tool electrode, resulting high *TWR*. As the feed rate increase the spark energy is more involved in material erosion, which reduces *TWR* and reaches to minimum. In the second phase, for further increase of feed rate from the optimum, the unflashed eroded materials cause unwanted spark with the tool, which results more tool wear. Thus high *TWR* is obtained. With the increase in capacitance large energy dissipated which produces stronger spark resulting high work material erosion. Higher spark energy produces higher amount of debris. These debris sticking on the workpiece, trapped in and causes unwanted spark. The unwanted sparks erodes materials from the tool electrode, which results high tool wear. Thus, higher capacitance results higher *TWR*. As significant amounts of spark energy are employed in sparking with debris, effectively a lower amount of work material is eroded. *TWR* is a ratio of tool wear and workpiece wear, so decreases in material removal mean increase in *TWR*.

3.1.3 Material Removal Rate

The developed *MRR* statistical quadratic model is:

$$\frac{1}{\sqrt{MRR}} = 16.85 - 3.68f - 1.24C - 0.070V + 0.28f^2 + 0.09C^2 + 0.04fC + 0.01fV \qquad (3.4)$$

Figure 3.5 shows the effect of feed rate-capacitance and feed rate-voltage on $\frac{1}{\sqrt{MRR}}$.

Therefore, the decrease of $\frac{1}{\sqrt{MRR}}$ with the increase of any of the factors means the increase in *MRR*. *MRR* increases with the increase in feed rate. For further increase in feed rate *MRR* starts falling slightly. As the feed rate increase, the spark energy is more involved in material erosion, which increases *MRR* till reaches to the optimum. For further increase of feed rate from the optimum, the unflashed eroded materials cause unwanted spark with the tool, which changes the tool shape making it uneven and rough. The spark discharge from this uneven tool results less *MRR*. With the increase in capacitance large energy dissipated which erodes more work materials with stronger spark. With the material erosion, the unflashed debris sticking on the workpiece is trapped in between the machining zone, which causes unwanted spark with the tool-electrode. Thus a great portion of discharge energy occupies with unwanted sparking, while the remaining erodes the work material. Hence, effectively a lower amount of work material is eroded.

3.2 Multiple response optimizations

This subsection discusses the optimization of four output responses, R_a, R_y, *TWR* and *MRR*. The developed non-linear models Equations (3.1) to (3.4) are used for multiple response optimization. Desirability function approach was used for optimization. The method finds operating conditions, e.g. feed rate, capacitance and voltage that provide the "most desirable" values of the responses, e.g. R_a, R_y, *TWR* and *MRR*. The following subsection describes the desirability function approach.
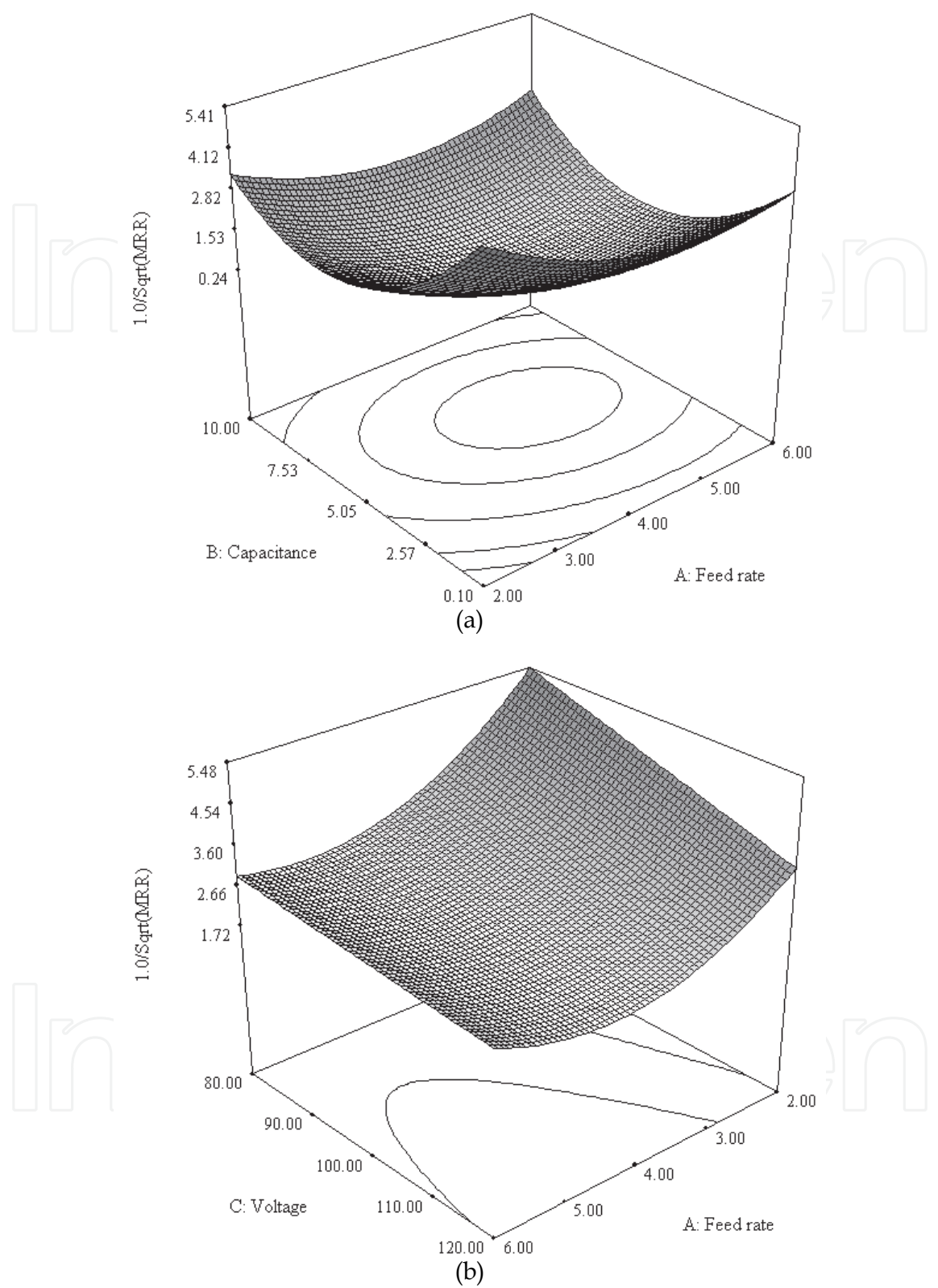
(a)

(b)

Fig. 3.5. Estimated response surface of *MRR* (mg/min): (a) $\dfrac{1}{\sqrt{MRR}}$ vs. *f* and *C* when *V* = 100 volts, (b) $\dfrac{1}{\sqrt{MRR}}$ vs. *f* and *V*, when *C* = 1.0 nF

3.2.1 Desirability function approach

In the analysis the objective function, $D(Y_i)$, called the desirability function, reflects the desirable ranges for each response $Y_i(x)$ (where, i = R_a, R_y, TWR, MRR). For each response, a desirability function $d_i(Y_i)$ assigns numbers between 0 and 1 to the possible values of Y_i.

$d_i(Y_i) = 0$ representing a completely undesirable value of Y_i and

$d_i(Y_i) = 1$ representing a completely desirable or ideal response value.

The individual desirabilities are then combined using the geometric mean, which gives the overall desirability D:

$$D = \sqrt[n]{(d_1 \times d_2 \times ..... \times d_n)} = (d_1 \times d_2 \times ..... \times d_n)^{\frac{1}{n}} \tag{3.5}$$

where n is the number of responses in the measure. From the equation (4.5) it can be noticed that if any response Y_i is completely undesirable ($d_i(Y_i) = 0$), then the overall desirability is zero. In this case, the geometric mean of overall desirability is as follows:

$$D = (d_{R_a} \times d_{R_y} \times d_{TWR} \times d_{MRR})^{\frac{1}{3}} \tag{3.6}$$

Depending on whether a particular response Y_i is to be maximized, minimized, or assigned a target value, different desirability functions $d_i(Y_i)$ can be used. In this case, R_a, R_y and TWR are needed to be minimized while MRR are needed to maximized. Following are the two desirability functions:

$$d_i(Y_i) = \begin{cases} 0 & if \quad Y_i(x) \leq L_i \\ \left(\dfrac{Y_i(x) - L_i}{T_i - L_i}\right)^s & if \quad L_i \leq Y_i(x) \leq T_i \\ 1.0 & if \quad Y_i(x) > T_i \end{cases} \tag{3.7}$$

$$d_i(Y_i) = \begin{cases} 1.0 & if \quad Y_i(x) < T_i \\ \left(\dfrac{Y_i(x) - U_i}{T_i - U_i}\right)^s, & if \quad T_i \leq Y_i(x) \leq U_i \\ 0 & if \quad Y_i(x) > U_i \end{cases} \tag{3.8}$$

where,

L_i = Lower limit values

U_i = Upper limit values

T_i = Target values

s = weight (define the shape of desirability functions)

Feed rate (µm/s)	Capacitance (nF)	Voltage (volts)	R_a (µm)	R_y (µm)	TWR	MRR (mg/min)	Desirability
4.79	0.10	80.00	0.04	0.34	0.044	0.08	88.06 %

Table 3.3. Values of process parameters for the optimization of R_a, R_y, TWR and MRR

Equation (3.7) is used when the goal is to maximize, while to minimize Equation (3.8) is needed. The value of s = 1 is chosen so that the desirability function increases linearly towards T_i. Table 3.3 shows the process parameters obtained after multiple response optimization. For the shown values of process parameters, it is 88.06% likely to get the R_a 0.04 µm, R_y 0.34 µm, *TWR* 0.044 and *MRR* 0.08 mg/min. Any other combination of the process parameters will either statistically less reliable or give poor results of at least one of the responses. The analysis was done by using computer software, Design Expert.

3.3 Verification of optimized values

Experiments were conducted to verify the result obtained from the multiple response optimization. The actual values obtained from the experiments are compared with the predicted values in Table 3.4. From the table it can be noticed that the predicted values of R_a shows no error with the actual, while TWR shows the maximum error. In 88.06% desirability, the percentages of error were found lesser for *TWR* and *MRR*. The bar charts of Figure 3.6 shows the comparison of predicted and actual values.

Desirability	Responses	Predicted	Actual	% Error
88.06%	R_a *(µm)*	0.04	0.04	0.00
	R_y *(µm)*	0.34	0.36	5.56
	TWR	0.044	0.053	16.98
	MRR (mg/min)	0.08	0.09	11.11

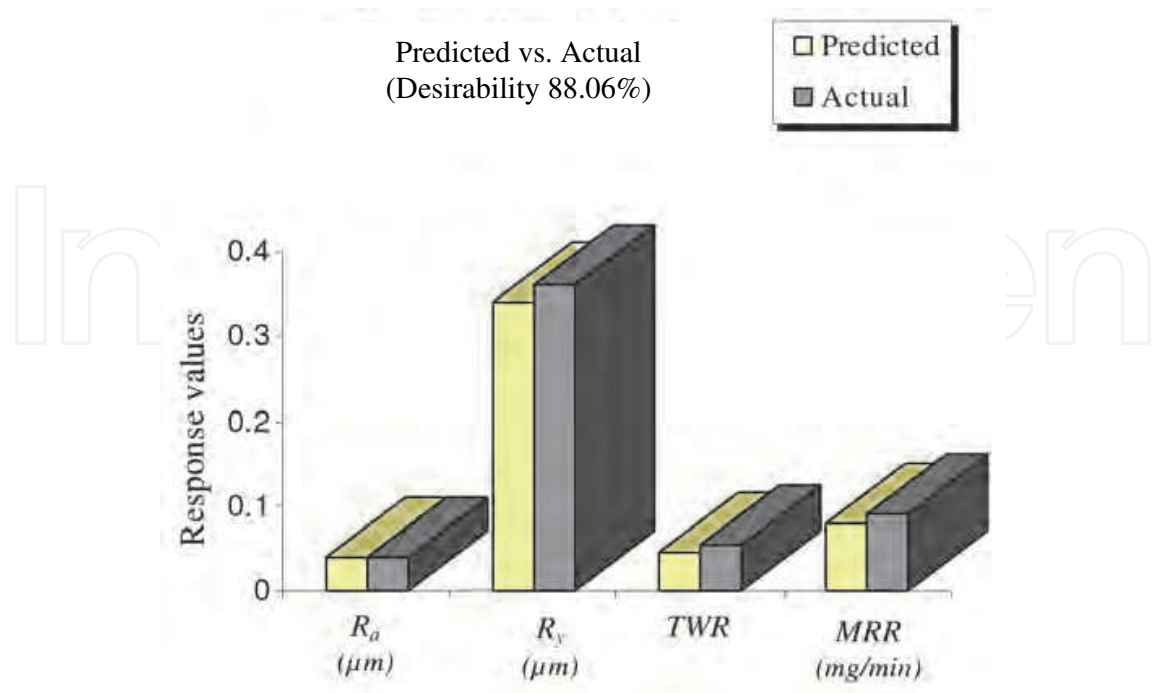Table 3.4. Verification of multiple response optimization

Fig. 3.6. Comparison of predicted vs. actual responses: (a) at desirability of 88.06%

4. Application of micro ed milling: Micro swiss-roll combustor mold

Micro swiss-roll combustor is a heat re-circulating combustor. It uses hydrocarbon fuels to generate high density energy. The advantage of a micro swiss-roll combustor is that it provides high density energy by reducing heat loss [Ahn and Ronney, 2005; Kim et al., 2007]. The generated heat inside the micro swiss-roll combustor is entrapped and re-circulated. Thus, high density energy is obtained. One of the challenges in micro combustor design is to reduce the heat loss. To reduce the heat loss by reducing surface-to-volume ratio, wall thickness should be as small as possible [Ahn et al. 2004]. The application of micro swiss-roll combustor includes portable electronics, such as cell phone, laptop, space vehicles, military uses, telecommunication, etc.
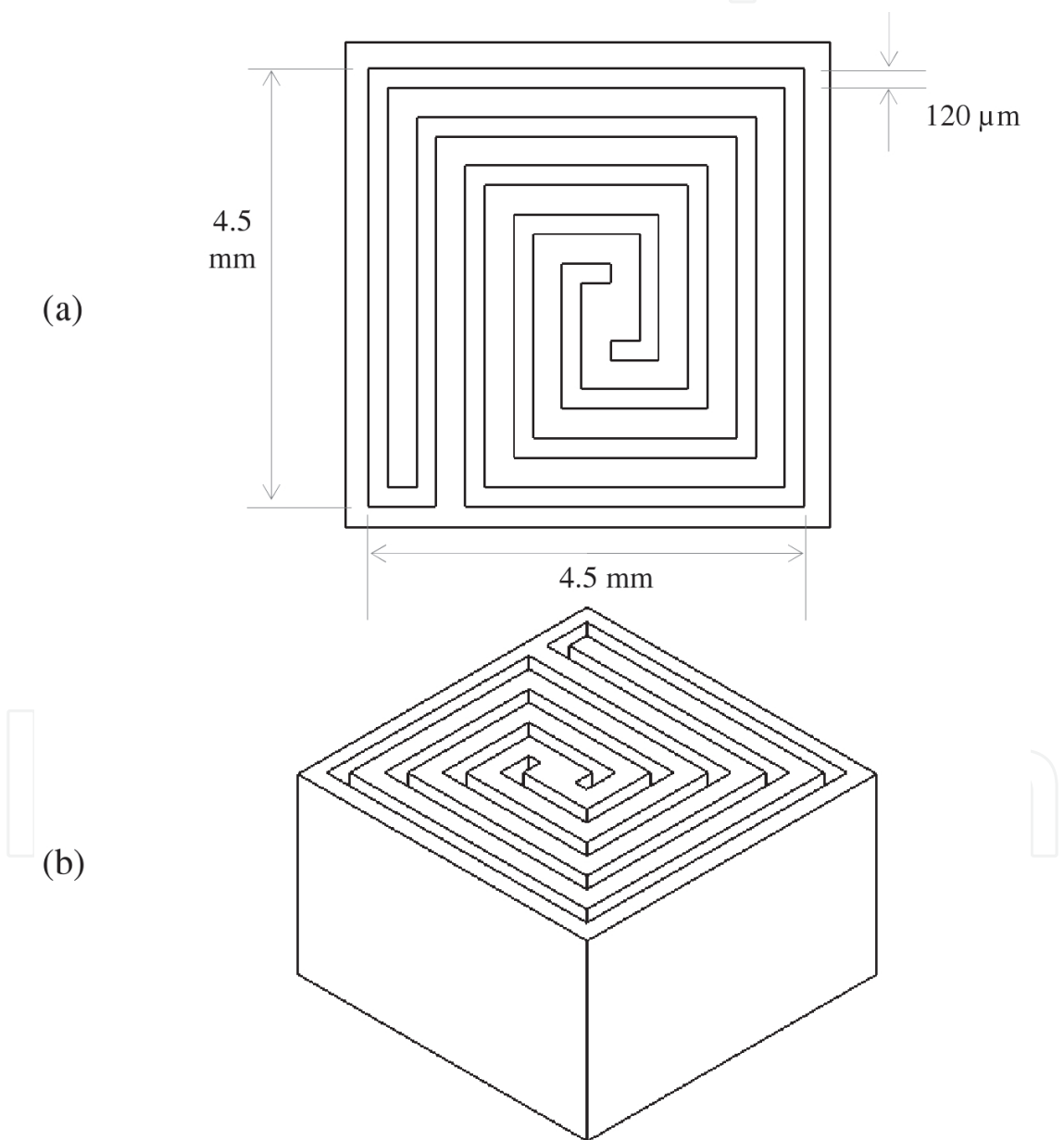
Fig. 4.1. Proposed design of micro swiss-roll combustor mold cavity (a) top view and (b) isometric view

The proposed design of the micro swiss-roll combustor mold cavity is shown in Figure 5.1. Beryllium-copper alloy (Protherm) was selected as the mold material, because of its high thermal conductivity, high heat and corrosion resistance. The microchannel of the mold cavity was fabricated by using a tungsten tool-electrode of 100 μm diameter. The minimum gap between two microchannels was 380 μm. The preliminary drawing and the numerical code (NC) of the design was generated by using CATIA V.5 R14 computer aided drafting software.

4.1 Fabrication of tool electrode by WEDG

Commercially available 300 μm diameter cylindrical tungsten rod was first dressed to 100 μm diameter by WEDG. Later this rod was used as a tool-electrode in micro ED milling to fabricate microchannels. Figure 4.2a illustrates the mechanism of WEDG. Figure 4.2b is the picture taken during the experiment and Figure 4.2c illustrates the SEM image of fabricated tool electrode. Computer numerical coding was used to control the size and shape of the required tool-electrode. The process parameters used are shown in Table 4.1. The parameter values were selected after preliminary studies.

Parameters	Values
Wire speed (mm/s)	20
Wire tension (%)	20
Capacitance (nF)	1
Voltage (volts)	100
Threshold (volts)	30
Polarity	Wire –ve
Spindle speed (rpm)	3000
Machining length (mm)	3
Di-electric medium	EDM-3 synthetic oil

The dimensions of the proposed micro-swiss roll combustor mold are:
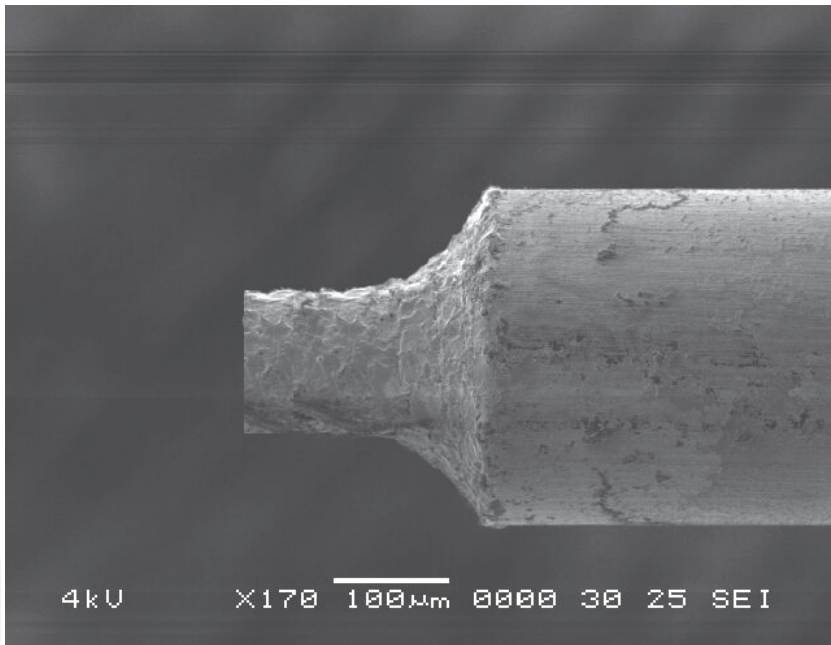*(length × width × depth)* = (4.5 mm × 4.5 mm × 1.0 mm)

Table 4.1. Experimental condition of WEDG for dressing of tool-electrode

Fig. 4.2. Schematic of tool-electrode dressing by WEDG
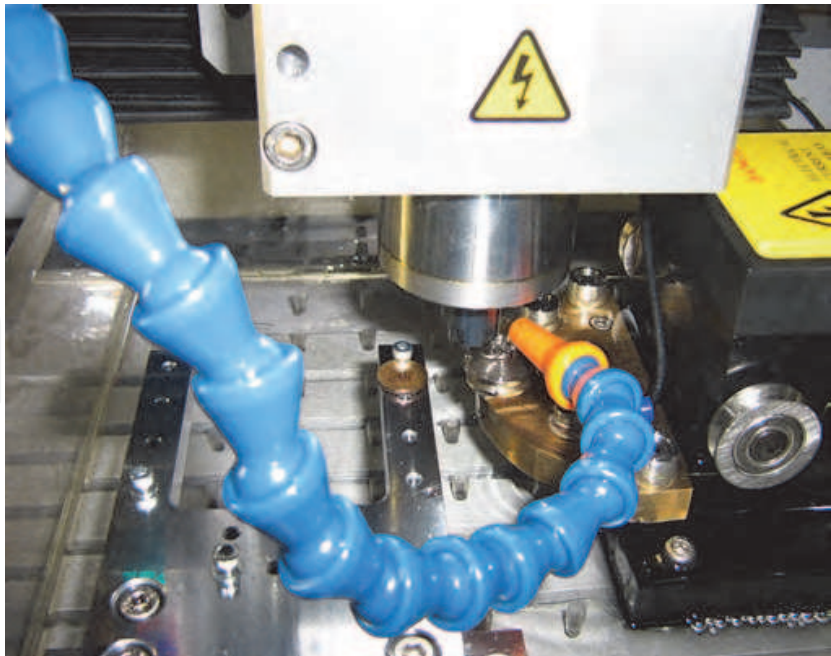
a)

b)

Fig. 4.3. Tool-electrode dressing by WEDG: (a) picture during WEDG and (b) SEM image of tool-electrode after dressing

4.2 Fabrication of micro mold cavity

The micro swiss-roll combustor mold cavity was fabricated by micro ED milling. Be-Cu alloy plate of 6 mm thickness was used as the workmaterial. The tool-electrode of 100 μm diameter was used, which produced microchannels of 120 μm width and 1 mm depth. Channel width comprises of the tool diameter and spark gap. Layer by layer approach was chosen to get better dimensional accuracy. The thickness of each layer was 200 μm. Figure

4.4 explains the layer by layer approach. The gap between two microchannels was 380 µm. After machining each 500 µm, the tool-electrode was dressed by WEDG to reduce the shape inaccuracy due to tool wear. The whole machining was done using computer numerical control. Figure 4.5a is the picture during experiments, Figure 4.5b shows the final product and Figure 4.5c shows the SEM micrographs of the window A in Figure 4.4b. The process parameters obtained from the multiple responses optimization were used in the microfabrication. The experimental condition is shown in Table 4.2.
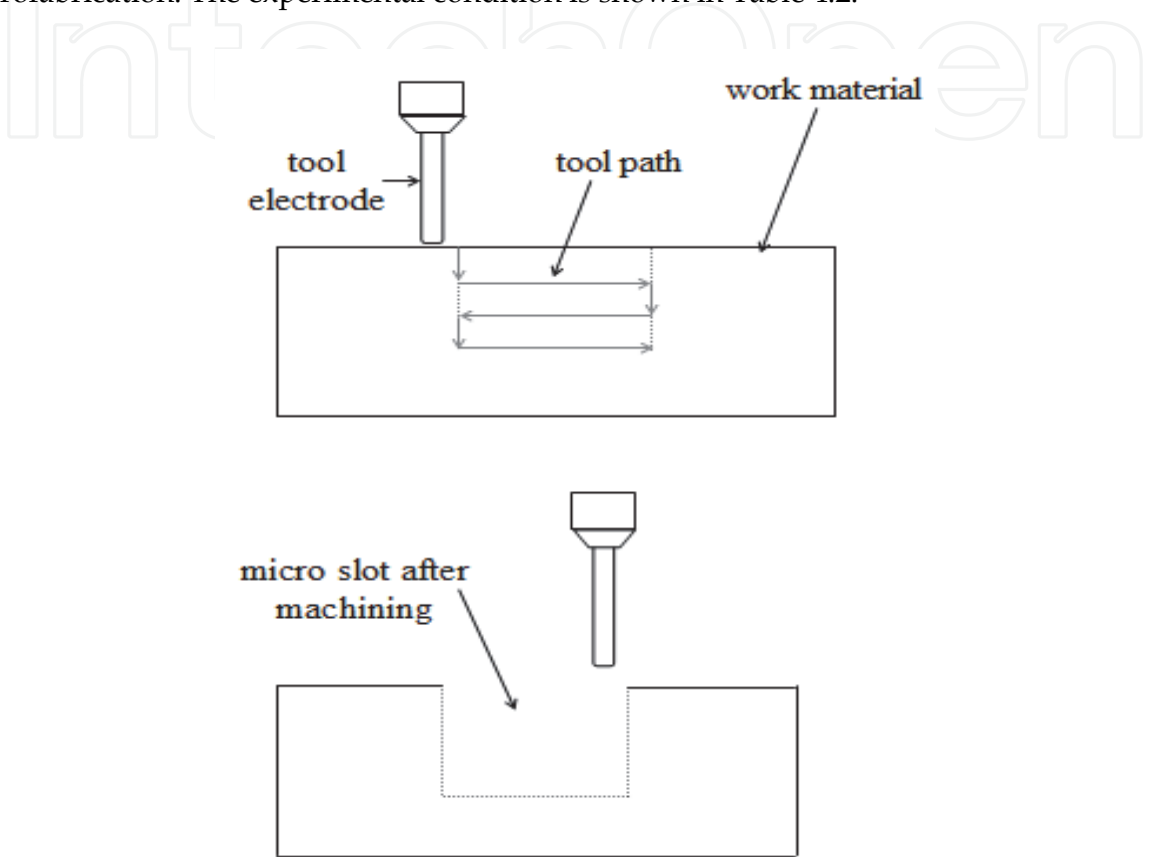
Fig. 4.4. Layer by layer machining: (a) before machining, b) after machining

Parameters	Values
Feed rate (µm/s)	4.79
Capacitance (nF)	0.1
Voltage (volts)	80
Threshold (volts)	30
Tool electrode dia (µm)	0.10
Spindle speed (rpm)	2000
Di-electric medium	EDM-3 synthetic oil
Depth per pass (µm)	200
Machining length per tool dressing (µm)	500

Table 4.2. Micro ED milling parameters for micro swiss-roll combustor mold
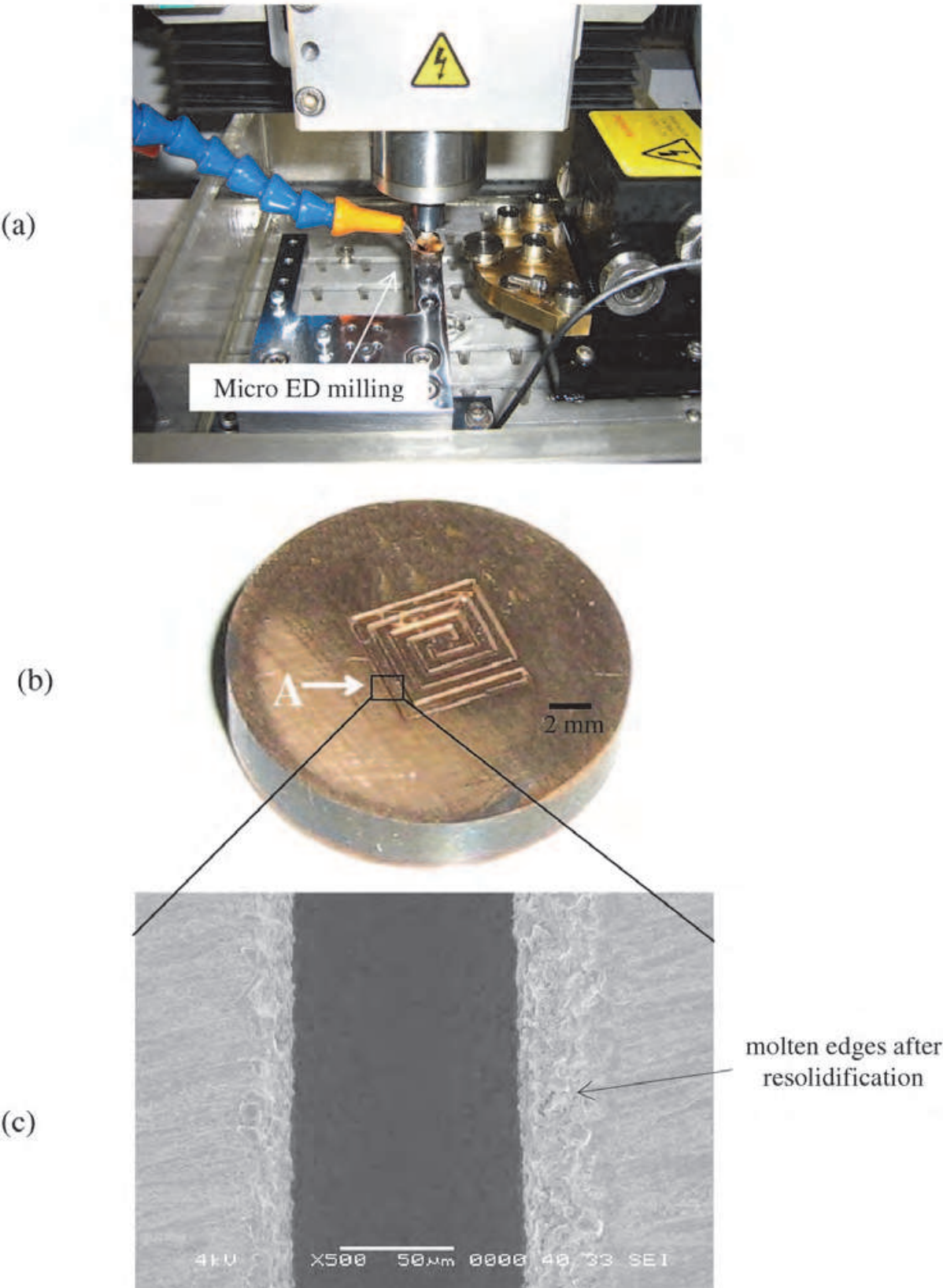
Fig. 4.5. Fabrication of micro swiss-roll combustor mold cavity by micro ED milling: (a) picture during micro ED milling, (b) fabricated micro swiss-roll combustor mold cavity, (c) SEM micrographs of window A in Figure 4.5 b.

5. Conclusion

Micro ED milling is shown as a potential fabrication technique for functional microcomponents. Influences of three micro ED milling parameters, feed rate, capacitance and voltage, were analyzed. Mathematical models were developed for output responses R_a, R_y, *TWR* and *MRR*. Analysis of multiple response optimization was done to get the best achievable response values. The micro ED milling process parameters obtained by the multiple response optimization were used in the fabrication of micro mold cavity. WEDG was used to dress the tool-electrode to a diameter of 100 μm. The final product was a micro swiss-roll combustor mold cavity. In brief, this research showed the followings:

1. Capacitance and voltage have strong individual influence on both the R_a and R_y, while the interaction effect of capacitance and voltage also affects the roughness greatly. Ususally higher discharge energy results higher surface roughness. The unflushed debris sticking on the workpiece causes higher R_a and R_y. At very high discharge energy the entrapped debris inside the plasma channel creates unwanted spark with the tool-electrode. Thus only a small portion of discharge energy involves in material erosion process, which results low R_a and R_y.
2. Capacitance and voltage plays significant role on *TWR* along with the interaction effect of feed rate and voltage. At high discharge energy large amount of debris are produced, which causes high *TWR* by generating unwanted sparks with the tool-electrode.
3. Feed rate, capacitance and voltage have strong individual and interaction effects on *MRR*. Usually, *MRR* is higher at high discharge energy. But the presence of high amount debris in the plasma channel often creates unwanted spark with the tool electrode. Thus only a portion of energy involves in workmaterial removal, which reduces *MRR*.
4. Multiple response optimization shows 88.06% desirability for minimum achievable values of R_a, R_y, *TWR* and maximum achievable *MRR*, which are 0.04 μm, 0.34 μm, 0.044, 0.08 mg/min respectively when the feed rate, capacitance and voltage are 4.79 μm/s, 0.10 nF and 80.00 volts respectively. The achieved R_a and R_y values are in the acceptable range for many MEMS applications.
5. The result of multiple response optimization was verified by experiment. The percentages of errors for R_a (0.0%), R_y (5.56%) at 88.06% desirability were found within the acceptable range. For *TWR* (16.98%) and *MRR* (11.11%), it was found relatively unsteady. Low resolution (0.1 mg) of electric balance could be a reason behind this.
6. A micro swiss-roll combustor mold cavity was fabricated by using the WEDG dressed tool. Optimized and verified micro ED milling process parameters were used for fabrication. The final product has the channel dimension of 0.1 mm.
7. Combination of micro ED milling and molding can be a suitable route for the mass replication of miniaturized functional components at a lower cost.

6. Acknowledgement

7. References

Ahn, J., Ronney, P. D., (2005). *Plastic mesocombustor.* 4th Joint U.S. Sections Meeting, Combustion Institute, Philadelphia, PA.
http://carambola.usc.edu/Research/MicroFIRE/PlasticMesoCombustors.pdf

Ahn, J. Eastwood, C., Sitzki, L., Ronney, P. D., (2004). *Gasphase and catalytic ombustion in heat-recirculating burners*. Proceedings of the Combustion Institute. (30).

Asad, A. B. M. A., Masaki, T, Rahman, M., Lim, H.S., Wong, Y.S., (2007). *Tool-based micro-machining*. Journal of Materials Processing Technology. (192–193) 204–211.

Bao, W. Y., Tansel, I. N., (2000). *Modeling micro-end-milling operations. Part 1: analytical cutting force model*. International Journal of Machine Tool and Manufacture. (40) 2155-2173.

Bao, W. Y., Tansel, I. N., (2000). *Modeling micro end milling operations. Part III: Influence of tool wear*. International Journal of Machine Tool and Manufacture. (40) 2193-2211.

Benavides, G. L., Bieg, L. F., Saavedra, M. P., and Bryce, E. A., (2002). *High aspect ratio meso-scale parts enabled by wire micro-EDM*. Microsystem Technologies (2002) (8) 395–401.

Cao D. M., Jiang, J., Yang, R., and Meng, W. J., (2006). *Fabrication of high-aspect-ratio microscale mold inserts by parallel µEDM*. Microsystem Technologies (2006) (12) 839–845.

Chen, Y., Mahdivian, S.M., (2000). *Analysis of electro-discharge machining process and its comparison with experiments*. Journal of Materials Processing Technology (104) 150-157.

Chen SL, Yan BH, Huang FY (1999) *Influence of kerosene and distilled water as dielectrics on the electric discharge machining characteristics of Ti-6Al-4V*. Journal of Materials Processing Technology (87)107–111.

Chiang, K. (2007). *Modeling and analysis of the effects of machining parameters on the performance characteristics in the EDM process of Al2O3+TiC mixed ceramic.* International Journal of Advanced Manufacturing and Technology. DOI 10.1007/s00170-007-1002-3

Chung, K. D., Kim, B. H. and Chu, C. N., (2007). *Micro electrical discharge milling using deionized water as a dielectric fluid.* Journal of Micromechanics and Microengineering (17) 867–874.

Dario, P., Carrozza, M. C., (1995). *Non-traditional technologies for micro fabrication*. Journal of Micromechanics and Microengineering. (5) 64-71.

DiBitonto, D. D., Eubank, P. T., Patel, M. R., Barrufet, M. A., (1989). *Theoretical models of the electrical discharge machining process 1. a simple cathode erosion model*. J Appl Phys. (66) 4095–4103.

Dryer, F. L., Yetter, R. A., (2006, November 10). *Research: chemical energy conversion and power generation at the microelectromechanical systems (MEMS) scale.* http://www.princeton.edu/~cml/html/research.html.

Ehmann, K. F., DeVor, R. E., and Kapoor, S. G., (2002). *Micro/meso-scale mechanical manufacturing- opportunities and challenges*. Proceedings of JSME/ASME International Conference on Materials and Processing. (1) 6-13.

Ekmekci, B., Elkoca, O., and Erden, A., (2005). *A comparative study on the surface integrity of plastic mold steel due to electric discharge machining*. Metallurgical and Materials Transactions B. (36B) 117-124.

Fleischer, J., Masuzawa, T., Schmidt, J., Knoll, M., (2004). *New applications for micro-EDM*. Journal of Materials Processing Technology. (149) 246–249.

Ghoreishi M, Atkinson J (2002) *A comparative experimental study of machining characteristics in vibratory, rotary and vibro-rotary electrodischarge machining*. Journal of Materials Processing Technology. (120) 374–384.

Han, F., Jiang, J., Yu, D., (2006) *Influence of machining parameters on surface roughness in finish cut of WEDM*", International Journal of Advanced Manufacturing Technology. DOI 10.1007/s00170-006-0629-9.

Her, M-G. and Weng, F-T., (2001) *Micro-hole machining of copper using the electro-discharge machining process with a tungsten carbide electrode compared with a copper electrode*. International Journal of Advanced Manufacturing and Technology (17) 715–719.

Hsu, T-R., (2002). *MEMS & microsystems- design and manufacture*. McGraw Hill.

Kim, N. I., Yokomori, T., Fujimori, T., Maruta, K., (2007). *Development and scale effects of small swiss-roll combustors*. Proceedings of Combustion Institute, doi :10.1016/ j.proci.2006.08.043.

Kim, Y. T., Park, S. J., Lee, S. J., (2005). *Micro/meso-scale shapes machining by micro EDM process*. International Journal of Precision Engineering and Manufacturing (6:2).

King, J. A., Tucker, B. D., Vogt, D., (1999). *Electrically and thermally conductive nylon 6,6*. Polymer Composites, (20) No. 5.

Lee, H. T., Tai, T. Y., (2003). *Relationship between EDM parameters and surface crack formation*. Journal of Materials Processing Technology (142) 676–683.

Lee, S. H., Li, X. P., (2001). *Study of the effect of machining parameters on the machining characteristics in electrical discharge machining of tungsten carbide*. Journal of Materials Processing Technology (115) 344–358.

Liao, Y. S., Huang, J. T., Chen, Y. H., (2004). *A study to achieve a fine surface finish in wire-EDM*. Journal of Materials Processing Technology. (149) 165–171.

Lim, H. S., Wong, Y. S., Rahman, M., Lee, M. K. E., (2003). *A study on the machining of high-aspect ratio micro-structures using micro-EDM*. Journal of Materials Processing Technology. (140) 318-325.

Lin, Y. C., Cheng, C. H., Su, B. L., Hwang, L. R., (2006). *Machining characteristics and optimization of machining parameters of SKH 57 high-speed steel using electrical-discharge machining based on taguchi method*. Materials and Manufacturing Processes. (21:8) 922 – 929.

Lin, Y., Matson, D. W., Kurath, D. E., Wen, J., Xiang, F., Bennett, W. D., Martin, P. *devices on polymer substrates for bioanalytical application* M., Smith, R. D., (1999). *Microfluidics*. Pacific Northwest National Laboratory.

Madou, M. J., (2002). *Fundamentals of micro fabrication*. The Science of Miniaturization. (2nd ed.) Florida, USA: CRC Press LLC.

Murali, M., and Yeo, H. S., (2004). *Rapid biocompatible micro device fabrication* by Micro Electro Discharge Machining. Biomedical Microdevices. (6:1) 41-45.

Mehfuz, R., Ali, M. Y. (2009). *Investigation of Machining Parameters for the Multiple Response Optimization of Micro Electro Discharge Milling*. The International Journal of Advanced Manufacturing Technology, (43), 264-275.

Orloff, J. (1997), *Handbook of charged particles optic*. CRC Press, New York, USA, 319-360.

Ozgedik, A. and Cogun, C., (2006). *An experimental investigation of tool wear in electric discharge machining*. International Journal of Advanced Manufacturing Technology (27) 488–500.

Pham, D. T., Dimov, S. S., Bigot, S., Ivanov, A., Popov, K., (2004). *Micro EDM- recent developments and research issues*. Journal of Materials Processing Technology. (149) 50-57.

Puertas, I., Luis, C. J., (2004). *A study of optimization of machining parameters for electrical discharge machining of boron carbide*. Materials and Manufacturing Processes, (19:6) 1041 – 1070.

Rajurkar, K. P., Pandit, S. M., (1986). *Formation and ejection of EDM debris*. ASME Trans Journal of Engineering Industry. (108) 22–26.

Ronney, P. D., (2003). *Analysis of non-adiabatic heatrecirculating combustors*. Combustion and Flame. (135) 421-439

Schoth, A., Fo¨rster, R., Menz, W., (2005). *Micro wire EDM for high aspect ratio 3D microstructuring of ceramics and metals*. Microsystem Technologies. (11) 250–253.

Snakenborg, D., Klank, H., Kutter, J. P., (2004). *Microstructure fabrication with a CO_2 laser system*. Journal of Micromechanics and Microengineering (14) 182-189.

Son, S. M., Lim, H. S., Kumar, A. S. and Rahman, M., (2007). *Influences of pulsed power condition on the machining properties in micro EDM*. Journal of Materials Processing Technology. (190) 73–76.

Uhlmann, E., Piltz, S., Jerzembeck, S., (2005). *Micro-machining of cylindrical parts by electrical discharge grinding*. Journal of Materials Processing Technology (160) 15–23.

Xingchao, Z., Yong, Z., Hao, T., Yong, L., Xiaohua, C., Guoliang, C., (2007). *Micro-electro-discharge machining of bulk metallic glasses*. Proceedings of HDP'07.
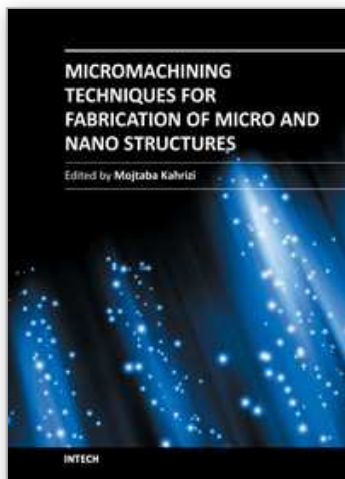
Micromachining Techniques for Fabrication of Micro and Nano Structures

Edited by Dr. Mojtaba Kahrizi

Micromachining is used to fabricate three-dimensional microstructures and it is the foundation of a technology called Micro-Electro-Mechanical-Systems (MEMS). Bulk micromachining and surface micromachining are two major categories (among others) in this field. This book presents advances in micromachining technology. For this, we have gathered review articles related to various techniques and methods of micro/nano fabrications, like focused ion beams, laser ablation, and several other specialized techniques, from esteemed researchers and scientists around the world. Each chapter gives a complete description of a specific micromachining method, design, associate analytical works, experimental set-up, and the final fabricated devices, followed by many references related to this field of research available in other literature. Due to the multidisciplinary nature of this technology, the collection of articles presented here can be used by scientists and researchers in the disciplines of engineering, materials sciences, physics, and chemistry.

How to reference

In order to correctly reference this scholarly work, feel free to copy and paste the following:

Mohammad Yeakub Ali, Reyad Mehfuz, Ahsan Ali Khan and Ahmad Faris Ismail (2012). Micro Eletro Discharge Milling for Microfabrication, Micromachining Techniques for Fabrication of Micro and Nano Structures, Dr. Mojtaba Kahrizi (Ed.), ISBN: 978-953-307-906-6, InTech, Available from: http://www.intechopen.com/books/micromachining-techniques-for-fabrication-of-micro-and-nano-structures/micro-eletro-discharge-milling-for-microfabrication

INTECH
open science | open minds